BJP BRITISH JOURNAL OF PHARMACOLOGY

BPS BRITISH PHARMACOLOGICAL SOCIETY

British Journal of Pharmacology (2010), 159, 919–927

0007-1188/10
www.brjpharmacol.org

RESEARCH PAPER

Thrombin activation of proteinase-activated receptor 1 potentiates the myofilament Ca^{2+} sensitivity and induces vasoconstriction in porcine pulmonary arteries

Jun Maki[1], Mayumi Hirano[1], Sumio Hoka[2], Hideo Kanaide[3] and Katsuya Hirano[1]

[1]*Division of Molecular Cardiology, Research Institute of Angiocardiology, Graduate School of Medical Sciences, Kyushu University, Fukuoka, Japan,* [2]*Department of Anesthesiology and Critical Care Medicine, Graduate School of Medical Sciences, Kyushu University, Fukuoka, Japan, and* [3]*International University of Health and Welfare, Fukuoka, Japan*

Background and purpose: Thrombus formation is commonly associated with pulmonary arterial hypertension (PAH). Thrombin may thus play an important role in the pathogenesis and pathophysiology of PAH. Hence, we investigated the contractile effects of thrombin and its mechanism in pulmonary artery.
Experimental approach: The cytosolic Ca^{2+} concentrations ($[Ca^{2+}]_i$), 20 kDa myosin light chain (MLC20) phosphorylation and tension development were evaluated using the isolated porcine pulmonary artery.
Key results: Thrombin induced a sustained contraction in endothelium-denuded strips obtained from different sites of a pulmonary artery, ranging from the main pulmonary artery to the intrapulmonary artery. In the presence of endothelium, thrombin induced a transient relaxation. The contractile effect of thrombin was abolished by either a protease inhibitor or a proteinase-activated receptor 1 (PAR_1) antagonist, while it was mimicked by PAR_1-activating peptide (PAR_1AP), but not PAR_4AP. The thrombin-induced contraction was associated with a small elevation of $[Ca^{2+}]_i$ and an increase in MLC20 phosphorylation. Thrombin and PAR_1AP induced a greater increase in tension for a given $[Ca^{2+}]_i$ elevation than that obtained with high K^+-depolarization. They also induced a contraction at a fixed Ca^{2+} concentration in α-toxin-permeabilized preparations.
Conclusions and implications: The present study revealed a unique property of the pulmonary artery. In contrast to normal arteries of the systemic circulation, thrombin induces a sustained contraction in the normal pulmonary artery, by activating PAR_1 and thereby increasing the sensitivity of the myofilament to Ca^{2+}. This responsiveness of the pulmonary artery to thrombin may therefore contribute to the pathogenesis and pathophysiology of PAH.
British Journal of Pharmacology (2010) **159,** 919–927; doi:10.1111/j.1476-5381.2009.00591.x; published online 28 January 2010

Keywords: pulmonary artery; thrombin; vasoconstriction; proteinase-activated receptor 1; Ca^{2+} sensitivity; myosin light chain phosphorylation

Abbreviations: CSS, cytosolic substitution solution; fura-2/AM, fura-2 acetoxymethyl ester; MLC20, 20 kDa myosin light chain; PAH, pulmonary arterial hypertension; p-APMSF, 4-aminidophenyl methane-sulphonyl fluoride; PAR, proteinase-activated receptor; PAR_1AP, PAR_1-activating peptide; PAR_4AP, PAR_4-activating peptide

Introduction

Pulmonary arterial hypertension (PAH) is a fatal disease with a progressive elevation of pulmonary arterial resistance and pressure. Pulmonary vasoconstriction thus plays a central role in PAH. Endothelin-1, 5-hydroxytryptamine and thromboxane A_2 have been suggested to be responsible for the vasoconstriction in PAH (Farber and Loscalzo, 2004). Despite therapeutic attempts with various vasodilators, the prognosis of PAH still remains unfavourable. The mechanism of pulmonary vasoconstriction thus still remains to be elucidated. The following observations suggest that thrombin plays a critical role in the vasoconstriction in PAH: thrombus formation and the thrombotic arteriopathy are commonly observed with PAH. Anticoagulant therapy alleviates the symptoms and improves the haemodynamic parameters in PAH (Johnson

Correspondence: Katsuya Hirano, Division of Molecular Cardiology, Research Institute of Angiocardiology, Graduate School of Medical Sciences, Kyushu University, 3-1-1 Maidashi, Higashi-ku, Fukuoka 812-8582, Japan. E-mail: khirano@molcar.med.kyushu-u.ac.jp
Received 10 August 2009; revised 4 October 2009; accepted 7 October 2009

et al., 2006a,b). However, the contractile effect of thrombin in pulmonary artery and its mechanism still remains to be investigated.

Thrombin not only contributes to thrombus formation as a coagulation factor, but it also exerts various vascular effects, including smooth muscle contraction (Coughlin, 2000; Hirano and Kanaide, 2003; Hirano, 2007b). A unique family of G protein-coupled receptors named proteinase-activated receptors (PARs) (Alexander *et al*., 2008) primarily mediate the cellular effects of thrombin (Coughlin, 2000; Macfarlane *et al*., 2001; Hollenberg and Compton, 2002; Ramachandran and Hollenberg, 2008). Thrombin cleaves the extracellular domain of PARs at a specific site, thereby unveiling a new N-terminus, which in turn acts as a tethered ligand and activates the receptor (Coughlin, 2000; Macfarlane *et al*., 2001; Hollenberg and Compton, 2002; Ramachandran and Hollenberg, 2008). Currently, four subtypes are known for PARs (Macfarlane *et al*., 2001; Hollenberg and Compton, 2002; Ramachandran and Hollenberg, 2008). Among them, PAR_1 and PAR_4 serve as the major signalling receptors for thrombin, while PAR_3 is thought to serve as a cofactor for the thrombin activation of PAR_1 or PAR_4, and PAR_2 is not activated by thrombin (Coughlin, 2000; Macfarlane *et al*., 2001; McLaughlin *et al*., 2007; Ramachandran and Hollenberg, 2008). The vascular effects of thrombin, in both endothelial cells and smooth muscle, have been intensively studied in the arteries of the systemic circulation. In vascular smooth muscle cells, thrombin induces contraction, cell migration, proliferation, hypertrophy and the production of the extracellular matrix, mainly by activating PAR_1 (Coughlin, 2000; Macfarlane *et al*., 2001; Hirano and Kanaide, 2003; Hirano, 2007b). However, the contractile effect of thrombin in normal arteries of the systemic circulation has only been shown in a few types of artery (Muramatsu *et al*., 1992; Ku and Zaleski, 1993; Godin *et al*., 1995), while the responsiveness to thrombin increases in vascular lesions such as those seen in atherosclerosis, balloon injury and subarachnoid haemorrhage (Ku and Dai, 1997; Fukunaga *et al*., 2006; Kai *et al*., 2007). Despite the fact that thrombotic arteriopathy is a common pathological observation in PAH, only a limited number of studies have so far addressed the contractile effect of thrombin in the pulmonary artery, while describing such an effect in small-sized arteries (Glusa and Paintz, 1994; Glusa *et al*., 1994). Therefore, the responsiveness to thrombin in the pulmonary artery and the mechanism for the thrombin-induced pulmonary artery vasoconstriction still remains to be elucidated.

The present study investigated the contractile response to thrombin at different sites of a pulmonary artery and then the mechanism underlying thrombin-induced contraction was determined with respect to intracellular Ca^{2+} signalling, the phosphorylation of 20 kDa myosin light chain (MLC20) and myofilament Ca^{2+} sensitivity. The present study focused mainly on the smooth muscle effect of thrombin in pulmonary artery. The contractile effect of thrombin was therefore investigated mainly in endothelium-denuded preparations. As a result, the present study demonstrated, for the first time, that thrombin induces a sustained contraction in the normal pulmonary artery by activating PAR_1 and thereby increasing myofilament Ca^{2+} sensitivity.

Methods

Tissue preparation of porcine pulmonary arteries

The main pulmonary arteries, the left pulmonary arteries and the proximal (segmental branch; ~4 mm in external diameter) and distal (subsegmental or more distal branch; approximately 1–2 mm in external diameter) intrapulmonary arteries were used to investigate the contractile effects of thrombin. Porcine pulmonary artery specimens were obtained at a local slaughterhouse immediately after the animals had been killed and brought back to the laboratory in ice-cold normal physiological salt solution (PSS). The intrapulmonary arteries were excised from the left upper lobes of the lung. After removal of the adventitia, the arterial segments of all types of pulmonary artery were opened longitudinally, and the endothelium was removed by rubbing with a cotton swab. Thereafter, they were cut into strips in a circular direction, measuring approximately 1 mm wide and 5 mm long. The removal of the functional endothelium was confirmed by the observation of the absence of the relaxant response to acetylcholine. When the contractile effect of thrombin was examined in the strips with an intact endothelium, special care was taken to avoid damaging the luminal surface of the strips. The cross-sectional area of the strips was estimated as described previously (Hirano *et al*., 1989). These preparations were referred to as 'intact' preparations regardless of the presence or absence of endothelium, in contrast to the α-toxin-permeabilized preparations.

Simultaneous measurement of cytosolic Ca^{2+} concentration ($[Ca^{2+}]_i$) and tension in fura-2-loaded intact strips of pulmonary artery

The strips were loaded with fura-2 by incubation for 3 h at 37°C in gassed (5% CO_2 and 95% O_2) Dulbecco's modified Eagle medium (DMEM) containing 5% fetal bovine serum and 25 μM fura-2 acetoxymethyl ester (fura-2/AM), as previously described (Sakihara *et al*., 1996). The strips were then washed to remove any of the fluorescence dye remaining in the extracellular space and equilibrated in normal PSS for at least 60 min at room temperature, before the experimental protocols were started. The fura-2-loaded strips were mounted vertically onto a force transducer, TB-612T (Nihon Koden, Tokyo, Japan), in a quartz organ bath (37°C) filled with normal PSS. The resting tension was adjusted to 250–300 mg, because this level was determined to be optimal to obtain the maximal tension development with 80 mM K^+-induced depolarization. During the equilibration period, the strips were stimulated with 80 mM K^+ a few times, to confirm reproducibility of the contractile response to 80 mM K^+-induced depolarization. The final response to 80 mM K^+ was used as a reference response in each strip. The changes in the fluorescence intensity of the fura-2–Ca^{2+} complex and the tension development were simultaneously monitored with a front-surface fluorometer, CAM-OF3, (JASCO, Tokyo, Japan), as previously described (Kanaide, 2006). The fluorescence intensities (500 nm) at 340 nm (F340) and 380 nm (F380) excitation were continuously monitored and their ratio (F340/F380) was recorded as an index of $[Ca^{2+}]_i$. The fluorescence ratio and tension development were expressed as a percentage; the values in normal

PSS (5.9 mM K^+) and those obtained with 80 mM K^+-PSS were assigned to be 0% and 100% respectively.

Tension measurement in α-toxin-permeabilized rings

For the study with the permeabilized preparations, distal intrapulmonary arteries with a relatively smaller size (1 mm in external diameter) were made into ring preparations measuring approximately 1 mm in width, and then were permeabilized with staphylococcal α-toxin, as previously described (Nishimura *et al.*, 1988) with minor modifications. The rings were briefly soaked in Ca^{2+}-free cytosolic substitution solution (CSS) and then permeabilized with 5000 U·mL^{-1} α-toxin in Ca^{2+}-free CSS for 40 min at 25°C. The rings were then treated with 10 μM A23187 in Ca^{2+}-free CSS for 20 min to deplete the intracellular Ca^{2+} stores. After being thoroughly washed in Ca^{2+}-free CSS, the arterial rings were mounted onto two tungsten wires bathed in a 200 μL droplet of Ca^{2+}-free CSS on a plastic plate by passing the tungsten wires through the lumen of the arterial ring. One of the wires was fixed and the other was connected to a force transducer U Gauge (Minebea, Tokyo, Japan). All tension measurements were performed in the presence of 300 nM Ca^{2+} and 10 μM GTP at 25°C. The contractile response to 10 μM Ca^{2+} was recorded as a reference response at the end of each measurement. The extent of tension development was expressed as a percentage, thus the values of the tension obtained in Ca^{2+}-free CSS (resting state) and 10 μM Ca^{2+} CSS (maximum contraction) were assigned to be 0% and 100% respectively.

Measurement of myosin light chain phosphorylation

The extent of the phosphorylation of MLC20 was analysed using the urea–glycerol gel electrophoresis technique (Persechini *et al.*, 1986), followed by the immunoblot detection of MLC20 (Zhou *et al.*, 1999). The strips were pulled to 1.2-fold of the resting length and pinned onto a rubber block to keep the resting load similar to that given in the tension measurement. At the indicated time after stimulation, the reaction was terminated by transferring the strip into a solution containing 90% acetone, 10% trichloroacetic acid and 10 mM dithiothreitol (DTT) prechilled by dry ice. The tissue specimens were then extensively washed and stored in acetone containing 10 mM DTT at –80°C. After the specimens had been air-dried to remove the acetone, the cellular protein was extracted in the sample buffer [8 M urea, 20 mM Tris (hydroxymethyl) aminomethane, 23 mM glycine, 0.004% bromophenol blue and 10 mM DTT] at room temperature for 1 h. The supernatant was then separated by electrophoresis on a 10% polyacrylamide gel containing 40% glycerol, followed by transfer to a nitrocellulose membrane in 10 mM Na_2HPO_4 (pH 7.6). Both the unphosphorylated and phosphorylated forms of MLC20 were detected by a mouse monoclonal anti-MLC20 antibody at 200-fold dilution (M-4401) and the horseradish peroxidase-conjugated anti-mouse IgM secondary antibody (×1000 dilution). The immune complex was detected using the enhanced chemiluminescence technique (ECL plus kit). The light emission was detected and analysed with ChemiDoc XRS-J and the computer programme Quantity One (BioRad). The percentage of the phosphorylated form in total MLC20 (sum of the unphosphorylated and phosphorylated forms) was calculated to indicate the extent of MLC20 phosphorylation.

Drugs, materials and solutions

Normal PSS consisted of 123 mM NaCl, 4.7 mM KCl, 15.5 mM $NaHCO_3$, 1.2 mM KH_2PO_4, 1.2 mM $MgCl_2$, 1.25 mM $CaCl_2$ and 11.5 mM D-glucose. PSS containing 80 mM K^+ was prepared by replacing NaCl with equimolar KCl. PSS was aerated with a mixture of 95% O_2 and 5% CO_2, with a resulting pH 7.4. The Ca^{2+}-free CSS consisted of 100 mM potassium methanesulphonate, 2.2 mM Na_2ATP, 3.38 mM $MgCl_2$, 10 mM creatine phosphate, 20 mM piperazine-N,N′-bis(2-ethanesulphonic acid) (PIPES), pH 6.8 and 10 mM EGTA. CSS containing the indicated concentrations of free Ca^{2+} was prepared by adding the appropriate amount of $CaCl_2$ to the Ca^{2+}-free CSS, while assuming the EGTA-Ca^{2+} binding constant to be 10^6 M^{-1} (Saida and Nonomura, 1978). Thrombin (bovine plasma; 1178 NIH U·mg^{-1} protein), α-toxin, GTPγS, GTP and 4-aminidophenyl methane-sulphonyl fluoride (p-APMSF) were purchased from Sigma. PAR_1 antagonist, SCH79797, was purchased from Tocris (Ellisville, MO, USA). Fura-2/AM and EGTA were obtained from Dojindo Laboratories (Kumamoto, Japan). PAR_1-activating peptide (PAR_1AP; TFLLR-NH_2) and PAR_4AP (AYPGKF-NH_2) were obtained from Bachem (Budendorf, Switzerland). Inactive control peptides for PAR_1AP (FTLLR-NH_2) and PAR_4AP (YAPGKF-NH_2) were synthesized by Rapid Multiple Peptide Synthesis Service, University of Calgary (Calgary, Alberta, Canada).

M-4401 was obtained from Sigma (St. Louis, MO, USA); the nitrocellulose membrane from BioRad (Hercules, CA, USA); the ECL plus kit from GH Healthcare (Buckinghamshire, UK).

Statistical analysis

Data are presented as the mean ± SEM. The numbers of experiments indicate the numbers of animals. Significant differences were statistically analysed by Student's unpaired *t*-test or either one-way or two-way ANOVA followed by Fisher's *post hoc* test. A *P*-value of less than 0.05 was considered to be statistically significant.

Results

Thrombin-induced contraction in the porcine pulmonary artery

Thrombin induced a sustained contraction in the absence of endothelium, in all intact strips obtained from the main pulmonary artery (19.0 ± 0.6 mm in external diameter), the left pulmonary artery (10.3 ± 0.3 mm in external diameter) and the proximal (3.8 ± 0.3 mm in external diameter) and distal intrapulmonary arteries (1.1 ± 0.1 mm in external diameter). The absolute values of the developed tension induced by both 1 U·mL^{-1} thrombin and 80 mM K^+-depolarization differed with the site of pulmonary artery, either with or without normalization by the cross-sectional area of strips (Figure 1A,B). The distal intrapulmonary artery yielded the maximal tension development per cross-sectional area. There was no significant difference in the relative responsiveness to

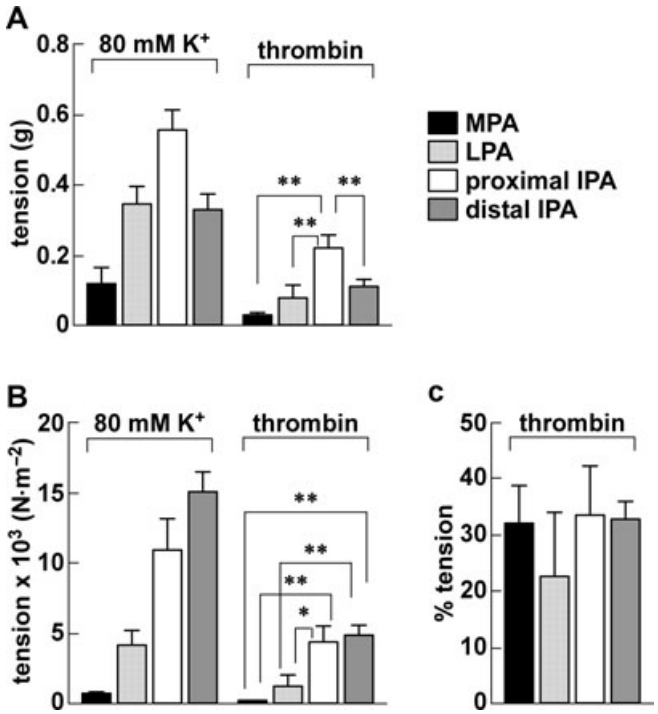

Figure 1 A comparison of the contractile responses to thrombin in strips prepared from different sites of a porcine pulmonary artery. (A,B) The absolute values of the developed tension induced by 80 mM K^+-depolarization and 1 U·mL^{-1} thrombin (n = 4) in the main pulmonary artery (MPA), left pulmonary artery (LPA), proximal and distal intrapulmonary artery (IPA) of the pigs, without (A) and with (B) normalization to cross-sectional area: 1.51 ± 0.41 mm^2 (MPA), 0.89 ± 0.14 mm^2 (LPA), 0.53 ± 0.07 mm^2 (proximal IPA) and 0.21 ± 0.02 mm^2 (distal IPA) (n = 4). (C) A summary of the relative contractile response to 1 U·mL^{-1} thrombin expressed as a percentage of that obtained with 80 mM K^+-depolarization. The data are expressed as the mean ± SEM. *P < 0.05; **P < 0.01.

thrombin among the different sites when the contractile response was compared with that obtained with 80 mM K^+-depolarization (Figure 1C).

In the distal intrapulmonary artery, 1 U·mL^{-1} thrombin induced a transient and a subsequent small sustained elevation of $[Ca^{2+}]_i$ in the absence of endothelium. The tension gradually developed and reached a maximum level at 13.7 ± 1.4 min (n = 3; Figure 2A). Thereafter, the contraction gradually decreased and eventually reached a plateau. This contractile effect of thrombin was completely abolished by pretreatment with a protease inhibitor, p-APMSF (Figure 2C). However, p-APMSF had no effect on the contractions induced by 80 mM K^+ or a PAR_1AP, TFLLR-NH_2 (data not shown). In the presence of endothelium, thrombin induced a transient relaxation during the U46619-induced sustained contraction in the distal intrapulmonary artery (Figure 2B); this was not observed in the absence of endothelium (data not shown). This endothelium-dependent relaxant effect of thrombin is thus consistent with the previous observations in the human pulmonary artery (Hamilton *et al*., 2001). However, the contractile effect of thrombin was not influenced by the presence of endothelium in the distal intrapulmonary artery (Figure 2D). The endothelium-denuded preparations were therefore used to investigate the mechanism of the contractile effect of thrombin in the following experiments.

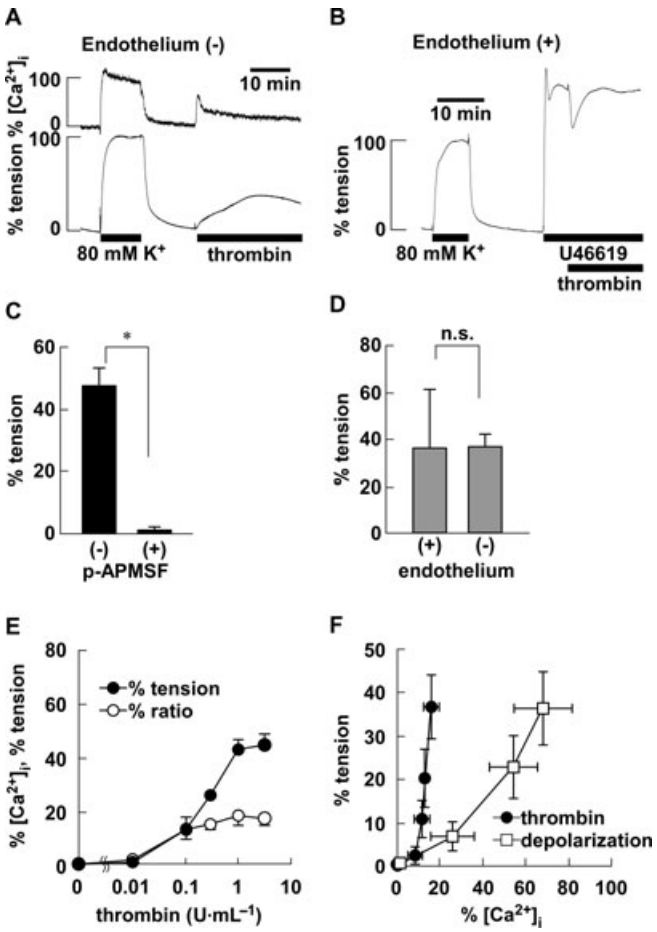

Figure 2 The effect of thrombin on the contraction induced in intact preparations of a porcine distal intrapulmonary artery, with and without endothelium. (A) Representative traces of the $[Ca^{2+}]_i$ elevation and the tension development induced by 1 U·mL^{-1} thrombin in the intact strip of the distal intrapulmonary artery. The levels of $[Ca^{2+}]_i$ and the tension were expressed as a percentage of those obtained with 80 mM K^+-depolarization. (B) Representative trace of three independent observations showing a relaxant effect of 1 U·mL^{-1} thrombin during the 100 nM U46619-induced contraction in the presence of endothelium. (C) The levels of tension developed 15 min after stimulation with 1 U·mL^{-1} thrombin in the presence and absence of a protease inhibitor, 4-aminidophenyl methane-sulphonyl fluoride (p-APMSF) (n = 5). Thrombin was pretreated with p-APMSF or vehicle (distilled water) for 10 min in a small concentrated volume, and then this mixture was applied to the 6 mL bathing solution so as to obtain final concentrations of 1 U·mL^{-1} thrombin and 10 μM p-APMSF. (D) A summary of the tension developed 15 min after stimulation with 1 U·mL^{-1} thrombin in the strips, with and without an intact endothelium (n = 3). (E) The concentration–response relationship for the thrombin-induced $[Ca^{2+}]_i$ elevations and tension development (n = 3). The levels of $[Ca^{2+}]_i$ and tension were evaluated at the maximum tension development. (F) The relationship between $[Ca^{2+}]_i$ and the size of the maximal contraction induced by different concentrations of thrombin (0, 0.01, 0.1, 0.3 and 1 U·mL^{-1}) was compared with that obtained by the stepwise increment of the extracellular Ca^{2+} concentrations (0, 0.025, 0.05, 0.125 and 0.25 mM) under 80 mM K^+-depolarization (n = 4). %$[Ca^{2+}]_i$ indicates % fluorescence ratio; the values obtained in normal physiological salt solution (PSS) and those obtained with 80 mM K^+-PSS were assigned to be 0% and 100% respectively. All data are expressed as the mean ± SEM. *P < 0.05; n.s., not significantly different.

A maximum elevation of both $[Ca^{2+}]_i$ and tension was observed with 1 U·mL^{-1} thrombin and higher concentrations. The concentration of thrombin required for the half maximal contraction (EC_{50} value) was 0.29 ± 0.04 U·mL^{-1} (Figure 2E). The sustained phase of the tension development was accompanied by a small elevation of $[Ca^{2+}]_i$ (Figure 2A,E). The evaluation of the $[Ca^{2+}]_i$–tension relationship revealed that thrombin induced a much greater contraction for a given elevation of $[Ca^{2+}]_i$ than 80 mM K^+-depolarization. This suggests that thrombin increases the sensitivity of the artery to Ca^{2+}(Figure 2F).

Involvement of PAR_1 in thrombin-induced contraction

PAR_1 and PAR_4 are the major signalling receptors for thrombin in the vascular smooth muscle (Hirano, 2007b). Their role in the thrombin-induced contraction was thus investigated as follows. TFLLR-NH_2, an activating peptide for PAR_1, induced a contractile response (Figure 3A–C), while its inactive control peptide, TFLLR-NH_2, had no significant effect (data not shown). FTLLR-NH_2 (10 μM) induced an initial transient contraction and an increase in $[Ca^{2+}]_i$, followed by sustained contraction with a small increase in $[Ca^{2+}]_i$ (Figure 3A). The removal of TFLLR-NH_2 from the bathing solution reversed the level of $[Ca^{2+}]_i$ and tension to the resting level (Figure 3A). Similar concentrations of TFLLR-NH_2 were required to induce both the initial transient and sustained phases of contraction (Figure 3B,C). The EC_{50} value for the contractile effect of TFLLR-NH_2 during the sustained phase was 1.56 ± 0.05 μM. TFLLR-NH_2 also induced a greater contraction for a given level of $[Ca^{2+}]_i$ than K^+-depolarization during the sustained phase but not at the peak of the contraction (Figure 3D,E).

A PAR_1 antagonist, SCH79797, substantially inhibited the contractions induced by both thrombin and TFLLR-NH_2, while it had no significant effect on the 80 mM K^+-induced contractions (Figure 4A). Furthermore, an activating peptide for PAR_4, AYPGKF-NH_2, induced no contractile effect at the same concentration of TFLLR-NH_2 required to induce maximal contraction or even higher concentrations (Figure 4B).

Ca^{2+}-sensitizing effect of thrombin and PAR_1AP in α-toxin-permeabilized preparations

The Ca^{2+}-sensitizing effect of thrombin and TFLLR-NH_2, as suggested by the $[Ca^{2+}]_i$–tension relationship in the intact preparations, was further evaluated in α-toxin-permeabilized rings. As shown in Figure 5A, thrombin induced a further increase in tension at a fixed Ca^{2+} concentration (300 nM). The maximum effect of thrombin was obtained at a concentration of 10 U·mL^{-1} and the EC_{50} value was 1.30 ± 0.02 U·mL^{-1} (Figure 5B). TFLLR-NH_2 also induced a further increase in tension at the fixed Ca^{2+} concentration (Figure 5C). The maximum effect of TFLLR-NH_2 was obtained at 30 μM, and the EC_{50} value was 1.72 ± 0.15 μM (Figure 5D). SCH79797 inhibited the contraction induced by thrombin in the α-toxin-permeabilized rings, whereas it had no effect on the GTPγS-induced contraction (Figure 5E).

Effect of thrombin on the phosphorylation of MLC20

Thrombin (1 U·mL^{-1}) significantly increased the level of MLC20 phosphorylation at 15 min, when the contraction reached the maximum (Figure 6A). This level of MLC20 phosphorylation was lower than that obtained with 80 mM K^+-depolarization. This disparity is consistent with the differences in developed tension (Figure 1). Furthermore, 10 μM TFLLR-NH_2 significantly increased the level of MLC20 phosphorylation when the contraction reached the maximum

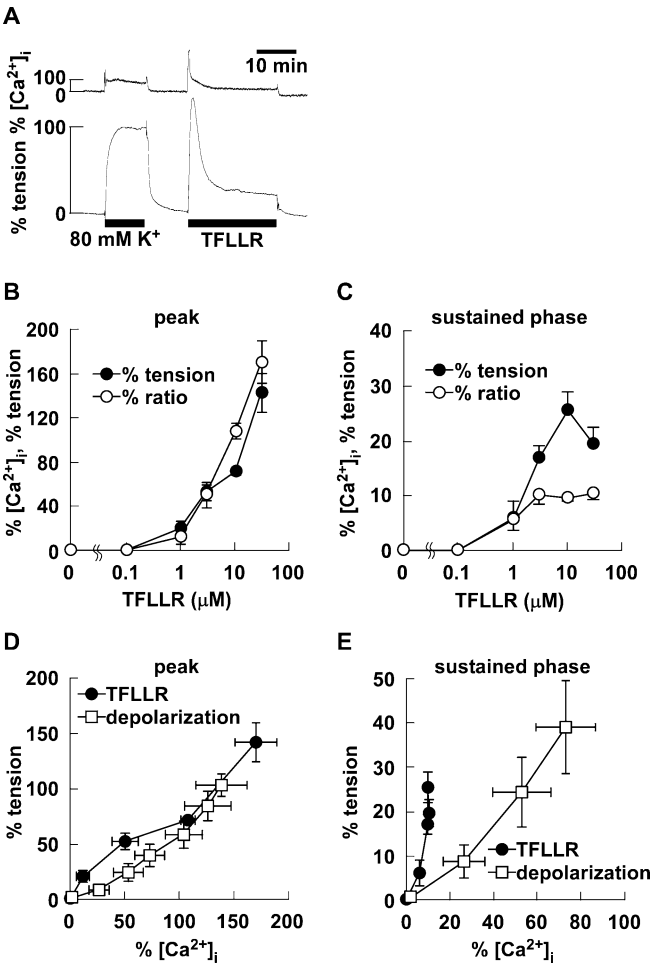

Figure 3 The contractile effect of proteinase-activated receptor 1-activating peptide (PAR_1AP) in intact preparations of a porcine distal intrapulmonary artery. (A) Representative traces of the $[Ca^{2+}]_i$ elevation and the tension development induced by 10 μM PAR_1AP, TFLLR-NH_2, in the intact strips of the distal intrapulmonary artery. (B,C) The concentration–response relationship (n = 4) for the TFLLR-NH_2-induced $[Ca^{2+}]_i$ elevation and tension development at the peak contraction (approximately 2 min after the stimulation) and sustained phase (15 min after stimulation). (D,E) The $[Ca^{2+}]_i$–tension relationships obtained at the peak (D) and the sustained phase (E) of the contraction induced by TFLLR-NH_2, (n = 4), were compared with those induced by 80 mM K^+-depolarization during stepwise increases in the extracellular Ca^{2+} concentrations (n = 5). The $[Ca^{2+}]_i$–tension relationships for the TFLLR-NH_2-induced contraction shown in (D) and (E) were reconstructed from the data shown in (B) and (C) respectively. The relationships between $[Ca^{2+}]_i$ and the level of tension developed for the 80 mM K^+-depolarization-induced contraction shown in (D) and (E) are those obtained with 0, 0.025, 0.05, 0.125, 0.25, 0.5, 1.25 and 2.5 mM Ca^{2+} and those obtained with 0, 0.025, 0.05, 0.125 and 0.25 mM Ca^{2+} respectively. %$[Ca^{2+}]_i$ indicates % fluorescence ratio; the values obtained in normal physiological salt solution (PSS) and those obtained with 80 mM K^+-PSS were assigned to be 0% and 100% respectively. All data are expressed as the mean ± SEM.

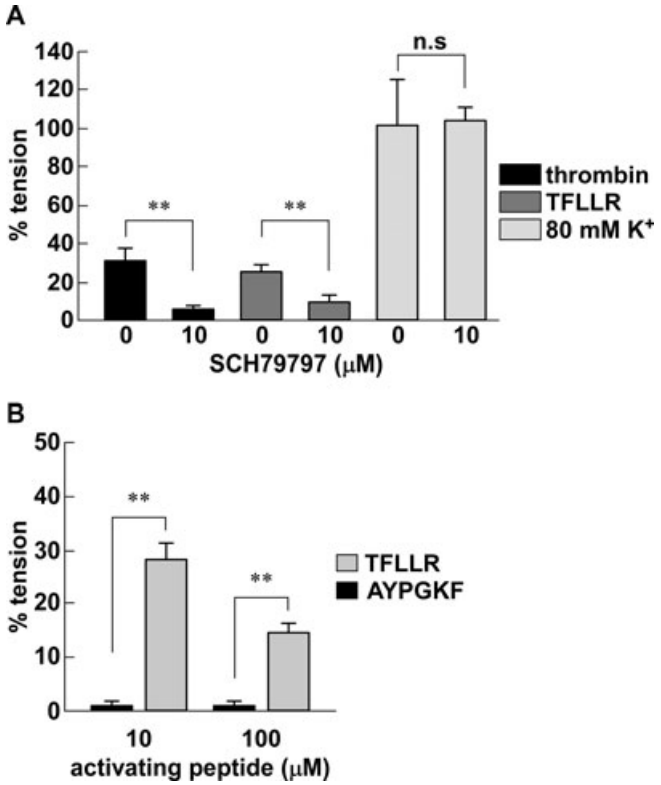

Figure 4 Role of proteinase-activated receptor 1 (PAR_1) in the thrombin-induced contraction in the intact strips of a porcine distal intrapulmonary artery. (A) The level of the tension developed 15 min after the stimulation of the intact strips with 1 U·mL^{-1} thrombin (n = 4), 10 μM TFLLR-NH_2 (n = 5) or 80 mM K^+-depolarization (n = 3) with or without pretreatment with 10 μM SCH79797. SCH79797 was applied 15 min before and during the contractile stimulation. (B) The levels of tension obtained 15 min after stimulation with 10 and 100 μM TFLLR-NH_2 or AYPGKF-NH_2 (n = 3). All data are expressed as the mean ± SEM. **P < 0.01; n.s., not significantly different.

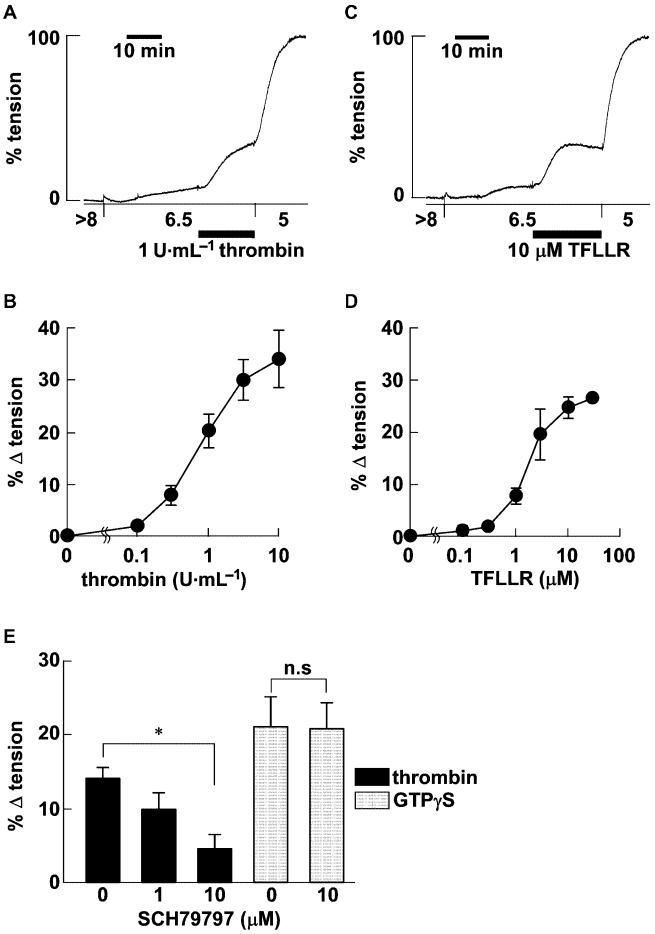

Figure 5 Contractile effect of thrombin and proteinase-activated receptor 1-activating peptide (PAR_1AP) in the α-toxin-permeabilized preparation of a porcine distal intrapulmonary artery. (A–D) Representative traces (A,C) and the concentration–response relationships (B,D) for the contractile effect of thrombin (A,B) and TFLLR-NH_2 (C,D) in the α-toxin-permeabilized rings (n = 4). (E) The level of maximal tension development obtained with 3 U·mL^{-1} thrombin (n = 5) or 10 μM GTPγS (n = 5), with or without 10 μM SCH79797 in the α-toxin-permeabilized rings. All data are expressed as the mean ± SEM. *P < 0.05; n.s., not significantly different.

(Figure 6B). Therefore, the contraction induced by thrombin was associated with an increase in MLC20 phosphorylation.

Effect of a Rho-kinase inhibitor on the thrombin-induced contraction

Rho-kinase plays an important role in the regulation of MLC20 phosphorylation and the sensitivity of the myofilament to Ca^{2+} in smooth muscle (Hirano, 2007a), as well as in the intracellular signal transduction following the activation of PAR_1 (Macfarlane *et al.*, 2001). The Rho-kinase inhibitor, Y27632, significantly inhibited the thrombin-induced contraction in the intact strips at 1 μM (34.4 ± 3.5%, n = 3) and 10 μM (2.6 ± 1.9%, n = 3) (Figure 7A). Y27632 also inhibited the contraction induced by 80 mM K^+-depolarization to 51.4 ± 9.1% (n = 3) and 27.9 ± 8.3% (n = 3) at 1 and 10 μM respectively. Y27632 (10 μM) inhibited the 80 mM K^+-depolarization-induced contraction (27.0 ± 10.7% of the control contraction seen in the absence of Y27632, n = 3) significantly (P < 0.01) less effectively than that induced by thrombin (5.6 ± 3.5% of the control contraction seen in the absence of Y27632, n = 3). Furthermore, Y27632 inhibited the thrombin-induced tension development in the α-toxin-permeabilized rings (Figure 7B), while having no effect on the GTPγS-induced tension development (data not shown). In contrast, 10 μM GF109203X, an inhibitor of protein kinase C, had no significant effect on the thrombin-induced contraction in the intact strips (data not shown).

Discussion

The present study demonstrated, for the first time, that thrombin induces a sustained contraction in normal pulmonary artery vasculature, ranging from the main pulmonary artery to the intraparenchymal artery. The findings also indicated that the relative responsiveness to thrombin was similar along the vasculature. Earlier studies have reported that thrombin induces a contraction in the small-sized pulmonary artery of pigs and have also shown that this contraction is dependent on the proteolytic activity of thrombin, which was

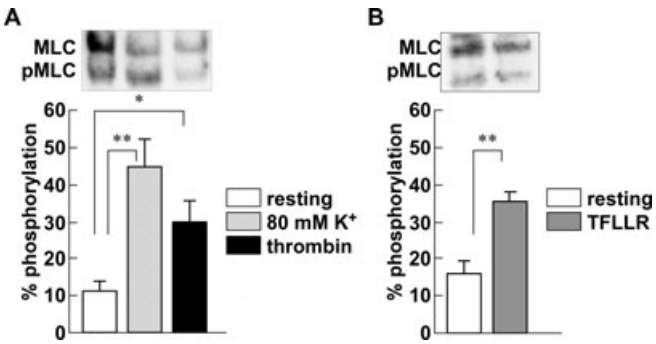

Figure 6 Effect of thrombin and PAR_1AP on the phosphorylation of MLC20 in a porcine distal intrapulmonary artery. Representative immunoblots and summaries of MLC20 phosphorylation obtained at the maximal contraction after the stimulation with 80 mM K^+-depolarization or 1 U·mL^{-1} thrombin (A) and 10 μM TFLLR-NH_2 (B) in intact strips. All data are expressed as the mean ± SEM [$n = 6$ in (A), 3 in (B)]. *$P < 0.05$; **$P < 0.01$. MLC, non-phosphorylated MLC20; MLC20, 20 kDa myosin light chain; PAR_1AP, proteinase-activated receptor 1-activating peptide; pMLC, mono-phosphorylated MLC20.

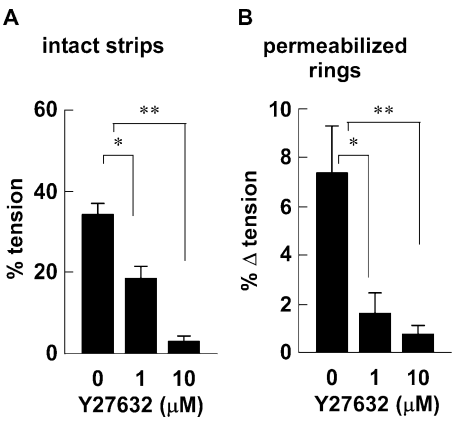

Figure 7 Effect of Y27632, a Rho-kinase inhibitor, on the thrombin-induced contraction in a porcine distal intrapulmonary artery. (A,B) The effect of Y27632 on the contraction obtained 15 min after stimulation with 1 U·mL^{-1} thrombin in the intact strips (A; $n = 3$) and that obtained with 3 U·mL^{-1} thrombin in the α-toxin-permeabilized rings (B; $n = 5$). The specimens were treated with 0, 1 and 10 μM Y27632 15 min before and during the stimulation with thrombin. All data are expressed as the mean ± SEM. *$P < 0.05$; **$P < 0.01$.

mimicked by a thrombin receptor-activating 14-mer peptide, thus suggesting the involvement of PAR_1 in the thrombin-induced contraction (Glusa and Paintz, 1994; Glusa *et al.*, 1994). However, the peptide used in this previous study can activate PAR_2 as well as PAR_1 (Hollenberg and Compton, 2002). Thus PAR_1 had not been conclusively demonstrated to be involved in this response. Furthermore, the mechanism of the thrombin-induced contraction remained to be elucidated. Hence, the results of the present study are the first to demonstrate that an increase in the sensitivity of the myofilament to Ca^{2+} during thrombin-induced contraction is the main mechanism for the sustained contraction, and we also present compelling evidence for the involvement of PAR_1.

The following observations convincingly suggest that PAR_1 plays a major role in mediating the contractile effect of thrombin in the pulmonary artery: the contractile effect of thrombin was abolished by the protease inhibitor, p-APMSF. PAR_1AP, TFLLR-NH_2, which specifically activated PAR_1, but not PAR_2 (Hollenberg and Compton, 2002), mimicked the contractile effect of thrombin, while PAR_4AP and the inactive control peptides for PAR_1AP and PAR_4AP had no effect. A PAR_1 antagonist inhibited the contractions induced by thrombin and PAR_1AP. Furthermore, unlike in the porcine renal artery, the contractile effect of thrombin in the pulmonary artery was shown not to be endothelium-dependent (Derkach *et al.*, 2000). These observations thus suggest that thrombin activates PAR_1 in smooth muscle, thereby exerting a direct contractile effect on the pulmonary artery.

Smooth muscle contraction is one of the vascular effects of thrombin activation of PAR_1 (Macfarlane *et al.*, 2001; Hirano, 2007b). However, the contractile effect of thrombin in the normal arteries of the systemic circulation has only been reported in a few types of artery (Muramatsu *et al.*, 1992, Ku and Zaleski, 1993; Godin *et al.*, 1995). On the other hand, endothelium-dependent relaxation is the most frequently reported vascular effect of thrombin in the normal arteries of the systemic circulation (Hamilton *et al.*, 2001; Macfarlane *et al.*, 2001). The endothelium-dependent relaxant effect of thrombin was also observed in porcine (present study) and human (Hamilton *et al.*, 2001) normal pulmonary arteries. In contrast, a direct contractile effect of thrombin on smooth muscle becomes apparent in vascular lesions, such as atherosclerosis, balloon injury and subarachnoid haemorrhage (Nelken *et al.*, 1992; Fukunaga *et al.*, 2006; Kai *et al.*, 2007). In this respect, the responsiveness to thrombin seen in our study is thought to be a unique characteristic of the pulmonary artery.

The contractions induced by thrombin and PAR_1AP were associated with increases in $[Ca^{2+}]_i$ and MLC20 phosphorylation. The sustained phase of the contraction was accompanied by a small increase in $[Ca^{2+}]_i$ in both cases. The tension development for a certain elevation of $[Ca^{2+}]_i$ during the sustained phase of the contraction was much greater than that seen during the 80 mM K^+-depolarization-induced contraction. Moreover, both thrombin and PAR_1AP induced a further increase in the contraction at fixed concentrations of Ca^{2+} in the α-toxin-permeabilized preparations. These observations suggest that the sensitivity of the myofilament to Ca^{2+} increases during the sustained phase of the contraction. It was also noted that PAR_1AP induced an initial transient contraction accompanied by a transient elevation of $[Ca^{2+}]_i$, which was absent during the response to thrombin. The $[Ca^{2+}]_i$–tension relationship during this transient contraction was similar to that obtained with 80 mM K^+-induced contraction. Therefore, Ca^{2+} sensitization is thought to contribute mainly to the sustained phase of the contraction. The reason for the difference in the initial response seen with thrombin and PAR_1AP remains unclear. It may be associated with a difference in the mode of receptor activation (Blackhart *et al.*, 2000) or a difference in the kinetics of drug diffusion.

Protein kinase C and Rho-kinase are the main mediators associated with Ca^{2+} sensitization (Somlyo and Somlyo, 2003; Hirano, 2007a). Staurosporine, a relatively broad-range inhibitor of protein kinase, has been shown to partially inhibit the thrombin-induced sustained contraction in pulmonary artery, thus suggesting the involvement of protein

kinases, including protein kinase C, in this contraction (Bretschneider *et al*., 1995). Rho-kinase has a Ca^{2+}-sensitizing effect in vascular smooth muscle (Somlyo and Somlyo, 2003; Hirano, 2007a), while PAR_1 activates the RhoA-Rho-kinase pathway (Coughlin, 2000). Our observations that Y27632 inhibited the thrombin-induced contraction in the intact preparations and in the α-toxin-permeabilized preparations are thus consistent with the possibility that Rho-kinase has a role in mediating the Ca^{2+}-sensitizing effect of thrombin.

In the normal human pulmonary artery vasculature, the arteries with an external diameter larger than ~1 mm are classified as elastic, while those with a diameter ranging from 0.1 to 1 mm are classified as muscular (Brenner, 1935). The sizes of the main and left pulmonary arteries of pigs are similar to those of the corresponding arteries in humans (Brenner, 1935). Both types of artery can be subjected to thrombus formation under pathological conditions. The elastic arteries are the site of thromboembolism in chronic thromboembolic PAH, while the muscular arteries are the site of thrombotic arteriopathy in idiopathic PAH (Bjornsson and Edwards, 1985; Dartevelle *et al*., 2004). Therefore, the findings of the present study suggest that the contractile responsiveness of the pulmonary artery towards thrombin contributes to the vasoconstriction of both types of artery in PAH. However, the role of PAR_1 in this pathological condition remains to be elucidated.

In conclusion, the present study revealed a unique property of the pulmonary artery. Thrombin does not induce smooth muscle contraction in many normal arteries of the systemic circulation (Hirano, 2007b). In contrast, the expression of PAR_1 is up-regulated and the contractile effect of thrombin becomes apparent in vascular lesions (Nelken *et al*., 1992; Ku and Dai, 1997; Fukunaga *et al*., 2006; Kai *et al*., 2007). In this respect, the responsiveness to thrombin seen in a normal artery is therefore a unique property of the pulmonary artery. We also elucidated some of the mechanisms underlying the contractile effect of thrombin in the pulmonary artery. Thrombin proteolytically activates PAR_1 in pulmonary arterial smooth muscle cells. PAR_1 activation induced both an elevation of $[Ca^{2+}]_i$ and increased the sensitivity of the myofilaments to Ca^{2+}. This latter effect was associated with MLC20 phosphorylation and might be attributed to activation of Rho-kinase. PAH is frequently associated with thrombotic pulmonary arteriopathy (Johnson *et al*., 2006a); therefore, this unique property of the pulmonary artery may contribute to the pathogenesis and pathophysiology of PAH.

Acknowledgements

We thank Mr Brian Quinn for linguistic comments and help with the manuscript. This study was supported in part by a Grant-in-Aid for Scientific Research (No. 205920883) from the Ministry of Education, Culture, Sports, Science and Technology, Japan and grants from Yokoyama Rinsho Yakuri Foundation.

Conflict of interest

None.

References

Alexander SP, Mathie A, Peters JA (2008). Guide to Receptors and Channels (GRAC), 3rd edition. *Br J Pharmacol* **153** (Suppl. 2): S1–S209.

Bjornsson J, Edwards WD (1985). Primary pulmonary hypertension: a histopathologic study of 80 cases. *Mayo Clin Proc* **60**: 16–25.

Blackhart BD, Ruslim-Litrus L, Lu CC, Alves VL, Teng W, Scarborough RM *et al*. (2000). Extracellular mutations of protease-activated receptor-1 result in differential activation by thrombin and thrombin receptor agonist peptide. *Mol Pharmacol* **58**: 1178–1187.

Brenner O (1935). Pathology of the vessels of the pulmonary circulation. *Arch Intern Med* **56**: 211–237.

Bretschneider E, Paintz M, Glusa E (1995). Inositol 1,4,5-triphosphate and protein kinase C are involved in thrombin- and trap-induced vascular smooth muscle contraction. *Agents Actions* **45**: 309–313.

Coughlin SR (2000). Thrombin signalling and protease-activated receptors. *Nature* **407**: 258–264.

Dartevelle P, Fadel E, Mussot S, Chapelier A, Herve P, de Perrot M *et al*. (2004). Chronic thromboembolic pulmonary hypertension. *Eur Respir J* **23**: 637–648.

Derkach DN, Ihara E, Hirano K, Nishimura J, Takahashi S, Kanaide H (2000). Thrombin causes endothelium-dependent biphasic regulation of vascular tone in the porcine renal interlobar artery. *Br J Pharmacol* **131**: 1635–1642.

Farber HW, Loscalzo J (2004). Pulmonary arterial hypertension. *New Engl J Med* **351**: 1655–1665.

Fukunaga R, Hirano K, Hirano M, Niiro N, Nishimura J, Maehara Y *et al*. (2006). Upregulation of proteinase-activated receptors and hypercontractile responses precede development of arterial lesions after balloon injury. *Am J Physiol Heart Circ Physiol* **291**: H2388–H2395.

Glusa E, Paintz M (1994). Relaxant and contractile responses of porcine pulmonary arteries to a thrombin receptor activating peptide (TRAP). *Naunyn Schmiedebergs Arch Pharmacol* **349**: 431–436.

Glusa E, Bretschneider E, Paintz M (1994). Contractile effects of thrombin in porcine pulmonary arteries and the influence of thrombin inhibitors. *Naunyn Schmiedebergs Arch Pharmacol* **349**: 101–106.

Godin D, Rioux F, Marceau F, Drapeau G (1995). Mode of action of thrombin in the rabbit aorta. *Br J Pharmacol* **115**: 903–908.

Hamilton JR, Moffatt JD, Frauman AG, Cocks TM (2001). Protease-activated receptor (PAR) 1 but not PAR2 or PAR4 mediates endothelium-dependent relaxation to thrombin and trypsin in human pulmonary arteries. *J Cardiovasc Pharmacol* **38**: 108–119.

Hirano K (2007a). Current topics in the regulatory mechanism underlying the Ca^{2+} sensitization of the contractile apparatus in vascular smooth muscle. *J Pharmacol Sci* **104**: 109–115.

Hirano K (2007b). The roles of proteinase-activated receptors in the vascular physiology and pathophysiology. *Arterioscler Thromb Vasc Biol* **27**: 27–36.

Hirano K, Kanaide H (2003). Role of protease-activated receptors in the vascular system. *J Atheroscler Thromb* **10**: 211–225.

Hirano K, Kanaide H, Nakamura M (1989). Effects of okadaic acid on cytosolic calcium concentrations and on contractions of the porcine coronary artery. *Br J Pharmacol* **98**: 1261–1266.

Hollenberg MD, Compton SJ (2002). International Union of Pharmacology. XXVIII. Proteinase-activated receptors. *Pharmacol Rev* **54**: 203–217.

Johnson SR, Granton JT, Mehta S (2006a). Thrombotic arteriopathy and anticoagulation in pulmonary hypertension. *Chest* **130**: 545–552.

Johnson SR, Mehta S, Granton JT (2006b). Anticoagulation in pulmonary arterial hypertension: a qualitative systematic review. *Eur Respir J* **28**: 999–1004.

Kai Y, Hirano K, Maeda Y, Nishimura J, Sasaki T, Kanaide H (2007). Prevention of the hypercontractile response to thrombin by

proteinase-activated receptor-1 antagonist in subarachnoid hemorrhage. *Stroke* **38**: 3259–3265.

Kanaide H (2006). Measurement of $[Ca^{2+}]_i$ in smooth muscle strips using front-surface fluorimetry. *Methods Mol Biol* **312**: 251–259.

Ku DD, Dai J (1997). Expression of thrombin receptors in human atherosclerotic coronary arteries leads to an exaggerated vasoconstrictory response *in vitro*. *J Cardiovasc Pharmacol* **30**: 649–657.

Ku DD, Zaleski JK (1993). Receptor mechanism of thrombin-induced endothelium-dependent and endothelium-independent coronary vascular effects in dogs. *J Cardiovasc Pharmacol* **22**: 609–616.

Macfarlane SR, Seatter MJ, Kanke T, Hunter GD, Plevin R (2001). Proteinase-activated receptors. *Pharmacol Rev* **53**: 245–282.

McLaughlin JN, Patterson MM, Malik AB (2007). Protease-activated receptor-3 (PAR3) regulates PAR1 signaling by receptor dimerization. *Proc Natl Acad Sci USA* **104**: 5662–5667.

Muramatsu I, Laniyonu A, Moore GJ, Hollenberg MD (1992). Vascular actions of thrombin receptor peptide. *Can J Physiol Pharmacol* **70**: 996–1003.

Nelken NA, Soifer SJ, O'Keefe J, Vu TK, Charo IF, Coughlin SR (1992). Thrombin receptor expression in normal and atherosclerotic human arteries. *J Clin Invest* **90**: 1614–1621.

Nishimura J, Kolber M, van Breemen C (1988). Norepinephrine and GTP-γ-S increase myofilament Ca^{2+} sensitivity in α-toxin permeabilized arterial smooth muscle. *Biochem Biophys Res Commun* **157**: 677–683.

Persechini A, Kamm KE, Stull JT (1986). Different phosphorylated forms of myosin in contracting tracheal smooth muscle. *J Biol Chem* **261**: 6293–6299.

Ramachandran R, Hollenberg MD (2008). Proteinases and signalling: pathophysiological and therapeutic implications via PARs and more. *Br J Pharmacol* **153** (Suppl. 1): S263–S282.

Saida K, Nonomura Y (1978). Characteristics of Ca^{2+}- and Mg^{2+}-induced tension development in chemically skinned smooth muscle fibers. *J Gen Physiol* **72**: 1–14.

Sakihara C, Nishimura J, Kobayashi S, Takahashi S, Kanaide H (1996). Direct inhibitory effect of chlorpromazine on smooth muscle of the porcine pulmonary artery. *Anesthesiology* **85**: 616–625.

Somlyo AP, Somlyo AV (2003). Ca^{2+} sensitivity of smooth muscle and nonmuscle myosin II: modulated by G proteins, kinases, and myosin phosphatase. *Physiol Rev* **83**: 1325–1358.

Zhou Y, Hirano K, Sakihara C, Nishimura J, Kanaide H (1999). NH_2-terminal fragments of the 130 kDa subunit of myosin phosphatase increase the Ca^{2+} sensitivity of porcine renal artery. *J Physiol* **516**: 55–65.